

Hardness Analysis, Hydrogen Test and Welding Size on Seamless Steel Pipes API 5L Gr.X65 PSL2 with Post Weld Heat Treatment (PWHT)

Journal of Mechanical Engineering, Science, and Innovation e-ISSN: 2776-3536 2025, Vol. 5, No. 2 DOI: 10.31284/j.jmesi.2025.v5i2.7968 ejurnal.itats.ac.id/jmesi

Pradhana Kurniawan¹, Darto², and Ubbayu Annaufal²

- ¹Department of Automotive Engineering Technology, Politeknik Negeri Madiun, Indonesia
- ²Department of Mechanical Engineering, Universitas Merdeka Malang, Indonesia

Corresponding author:

Pradhana Kurniawan

Department of Automotive Engineering Technology, Politeknik Negeri Madiun, Madiun, 63162, Indonesia

Email: pradhanakurniawan@pnm.ac.id

Abstract

Seamless steel pipes are often used in oil and gas pipeline applications that work at high pressure, so the welding process is very important to ensure safety. This study aims to analyze the hardness, hydrogen test and welding size of seamless steel pipes that undergo post weld heat treatment (PWHT) process. The pipe diameter dimension is 6 inches with API 5L Gr.X65 PSL2 type. The experimental method begins with the PWHT process by heating to a temperature of 625 °C with a holding time of 1 hour 10 minutes then slowly cooled with a cooling rate of 154 °C / hour. Specimens after PWHT were analyzed for hardness, hydrogen testing and welding size simulation. The test results showed a decrease in hardness in the base metal, Heat Affected Zone (HAZ), and weld center. Position 0 ° ranges from 126-174 HRB, position 120 ° produces a value of 122 - 143 hardness rockwell B (HRB) and position 270 ° has a value of 133-154 HRB. The decrease in hardness occurs due to the tempering process which reduces residual stress. The pressure generated in the hydrogen test does not exceed the yield strength of the API 5L Gr.X65 PSL2 pipe material, which is 65,300 psi. The maximum weld size simulation results are produced with a value of 6,448 mm and a minimum value of 1,572 mm. The maximum value is used as a reference in welding to produce a safe connection.

Keywords: Hardness, hydrotest, welding size, seamless steel, post weld heat treatment

Received: July 11, 2025; Received in revised: September 30, 2025; Accepted: October 4, 2025

Handling Editor: Frizka Vietanti

INTRODUCTION

Seamless pipe is made from solid steel sheets or bars formed into billets [1]. The billets are then heated and pressed into a piercing rod-shaped mold to create a hollow tube or shell. Seamless pipe has advantages, including its ability to withstand high pressures and greater efficiency [2]. These advantages make it frequently used in gas pipelines, oil pipelines, hydraulic cylinders, and the hydrocarbon industry [1], [2], [3].

Shielded Metal Arc Welding (SMAW) is a common welding method for seamless steel pipes due to its versatility, flexibility, and low cost [4]. SMAW welding on seamless pipes requires careful attention due to the high pressure involved. Imperfect welds can result in hot cracks and residual stress, which directly reduce the strength of the joint [5]. Hot cracks and residual stress occur during high-temperature changes during the welding process [6], [7]. If not identified early, these conditions can lead to component failure [8], [9].

One method for minimizing cracking and residual stress is PWHT [10], [11]. PWHT is performed by reheating the welded pipe section at a temperature of approximately 580°C to 620°C with a holding time of 1 hour for every 25 mm of pipe thickness. After this process, slow cooling is performed to prevent the generation of new stresses [10], [12]. Previous research has shown that PWHT is effective in stabilizing the fabric against distortion, reducing residual stress and the risk of brittle fracture, thereby improving the mechanical properties of welded joints [13]. These improvements include hardness, toughness, corrosion resistance, and increased safety [14].

Research from Kusminah et al [15] examined API 5L X65 pipes that underwent PWHT using the Submerged Arc Welding (SAW) spiral method. The analysis focused on the effect of PWHT temperature variations on residual stress and corrosion. The research results showed that the relative residual stress value decreased (<2%), in addition, indications of hydrogen cracking were also seen but were still within the NACE MR0175 standard. Furthermore, research from Ravikiran et al [16] analyzed the crystallography and microstructure of API X65 pipes that underwent PWHT after high-frequency electric resistance welding (HF-ERW). The results indicated that the dominant texture orientation of PWHT was rotated cube and Goss and directly succeeded in reducing the intensity of adverse textures in the material. Research from Wang et al [17] related to PWHT on X80 steel pipes welded using Gas Metal Arc Welding (GMAW). The analysis carried out was related to Crack Tip Opening Displacement (CTOD) and its relationship with residual stress. The results showed that PWHT treatment at a temperature of 580°C with a holding time of 1 hour did not increase CTOD in the CGHAZ (Coarse-Grained Heat Affected Zone) but reduced residual stress. Finally, Alipooramirabad et al [18] studied PWHT on API 5L X70 pipes with Modified Short Arc Welding and Flux Cored Arc Welding. Residual stresses were measured using neutron diffraction. The results indicated that the initially high residual stress (650 MPa) after PWHT treatment could be drastically reduced to 144 MPa.

Previous research related to PWHT has mostly focused on API X65 SAW spiral joints with residual stress and corrosion analysis [15], API X65 HF-ERW with crystallographic texture studies [16], X80 with GMAW through CTOD evaluation [17], and X70 with MSAW/FCAW using neutron diffraction measurements [18]. The research emphasis is still limited to residual stress, corrosion and microstructure analysis. Until now, there are still very limited reports related to API 5L Gr.X65 PSL2 seamless pipe research using the SMAW method, especially those integrating hardness analysis, hydrogen test (hydrotest), and numerical simulation of weld size in evaluating the effect of PWHT on the safety and efficiency of welded joints in high-pressure pipes.

METHODS AND ANALYSIS

The methods used in this study were experiments and simulations. Experiments

Tablel 1. Chemical Composition of API 5L Gr.X65 PSL2 Material

| Elements | C | Mn | Si | Ni | Cr | Мо | Cu | Р |
|----------|------|-----|------|-----|-----|------|------|-----|
| Max (%) | 0.11 | 1.2 | 0.35 | 0.3 | 0.3 | 0.15 | 0.35 | 0.2 |

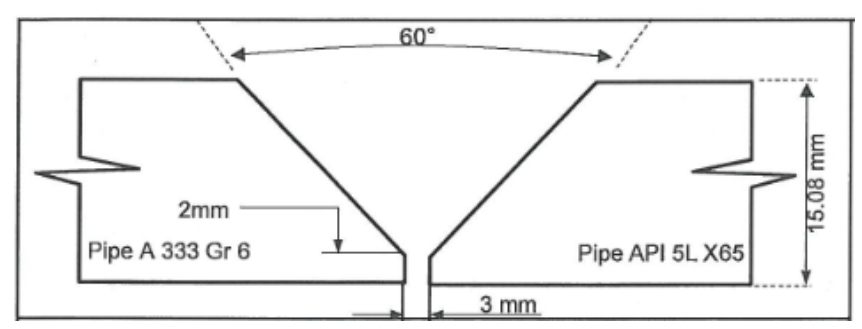


Figure 1. Welding Specimen with Single V Groove Method

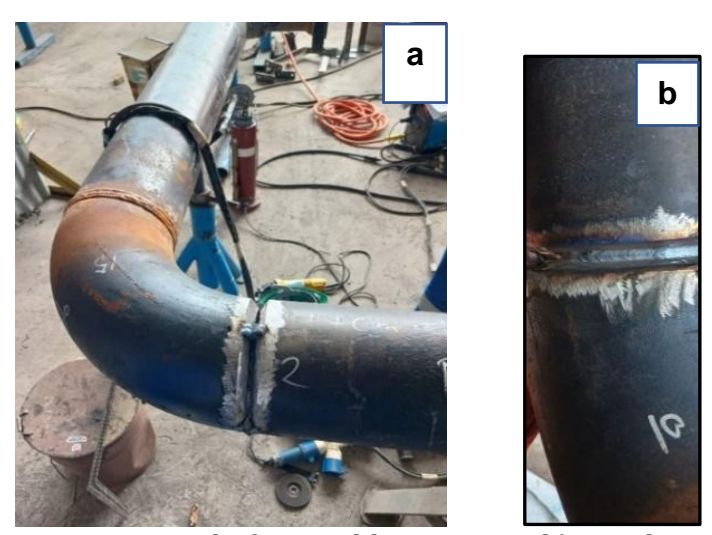


Figure 2. a) Fit Up Process before Welding Process b) Results After Welding

included material preparation, PWHT treatment, hardness testing, and hydrogen testing. Simulations served as supplementary data, starting with pipe design, material selection based on experiments, welding connector selection, meshing, boundary conditions, and results (welding size, equivalent von misses).

Material

The material used in this study was seamless steel pipe with type API 5L Gr.X65 PSL2. The pipe size has a diameter of 6 inches with a thickness of 15.08 mm. The results of the chemical composition test can be seen in Table 1. The chemical composition in Table 1 is obtained from the manufacturing certificate of API 5L Gr. X65 PSL2 product.

Welding Preparation

The pipe specimen to be welded was cut and formed into a single v groove with a slope of 60°C. Details of the size dimensions can be seen in Figure 1. The specimens prepared were 3, coded A, B and C. Before welding, a fit-up process was carried out as in Figure 2. Welding used SMAW with an E7018 electrode type, 4.0 mm diameter, and a current of 180 A.

PWHT Process

The welded pipe is then immediately subjected to PWHT in a portable furnace. This treatment aims to minimize the occurrence of hydrogen cracking by quickly removing the diffusible hydrogen content. The PWHT process was carried out using a portable furnace

(Cooperheat 6, Cooperheat Equipment Ltd., UK). Heating was carried out in stages to a temperature of 626° C with a holding time of 1 hour and 10 minutes, after which it was slowly cooled at a cooling rate of 155° C/hour. This graph can be seen in Figure 3. Temperature uniformity was controlled by rotating the thermocouple at 0° , 120° , and 240° around the pipe circumference. The pipe was then slowly rotated in a portable furnace before holding time was applied.

Hardness Test

Hardness testing using a portable hardness tester Krisbow brand with model number 10238107. 5 points were taken in the weld area and then points were taken at rotations of 0°, 120° and 240°. The position of the weld area points can be seen in Figure 4, while the rotation points can be seen in Figure 5. Figure 4 at points 1 and 5 show the base metal, points 2 and 4 are the HAZ area, while point 3 is the center of the weld area.

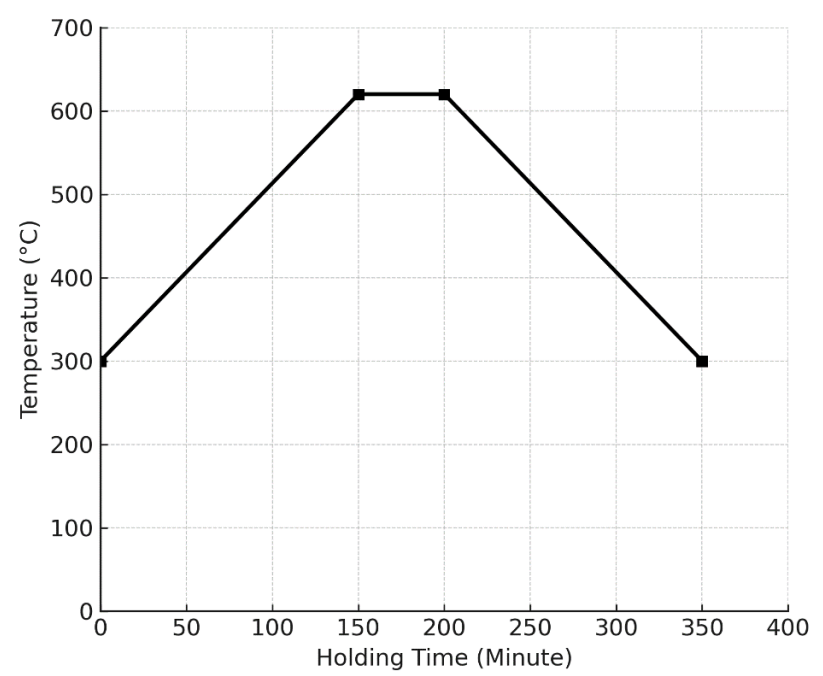


Figure 3. PWHT Process

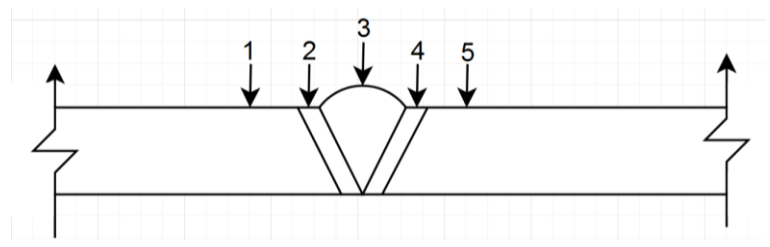


Figure 4. Points on the Weld Area

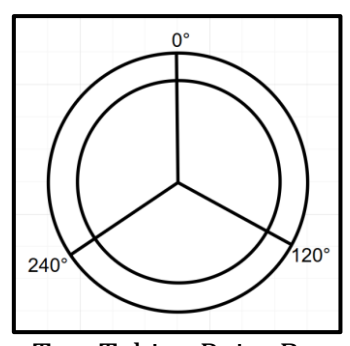


Figure 5. Hardness Test Taking Point Based on Angle Rotatio

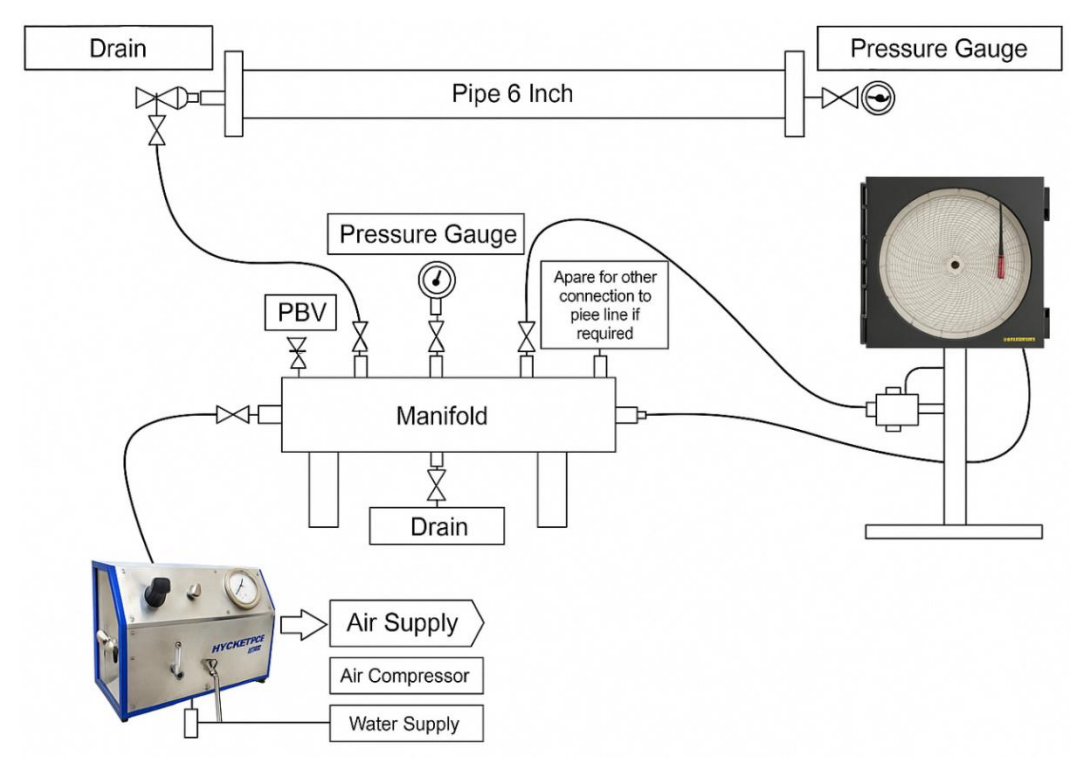


Figure 6. Hydrogen Test Scheme

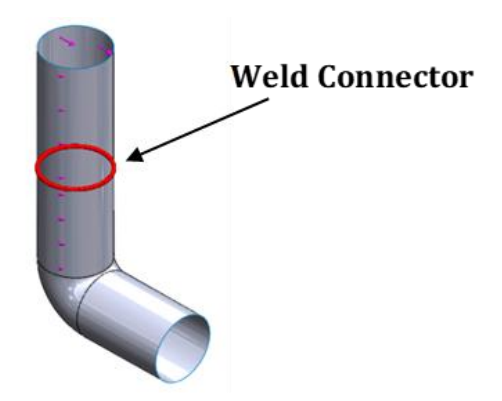


Figure 7. Weld Connector Position

Hydrogen Test

The hydrogen test uses a pressure of 1.5 times the maximum operating pressure for a period of 30 minutes to 1 hour. The hydrogen test schematic is shown in Figure 6. The hydrogen level is increased gradually from 50%, 75%, and 100%. Hydrogen testing refers to the standardization of ASME B31.12 (Hydrogen Piping and Pipeline Code).

Welding Size Simulation

Simulation testing aims to analyze the recommended pipe weld size limits to prevent over-welding and their effect on stress concentration compared to the yield strength of the pipe material. Welding size simulation using Solidworks 2018 software. The meshing type uses tetrahedral, global element size 3 mm, control at the elbow section with element size 1.5 mm. Mesh quality uses a Jacoban ratio ≥ 0.3 . Convergence is assessed based on the highest stress results <5% between consecutive mesh levels. The connector used is a single-sided groove (Figure 7), weld sizing uses American standards with E70 electrodes. A fixed support was applied at the inlet end of the pipe, while a longitudinal force was applied at the outlet end. The applied force was calculated from the design pressure and the pipe's cross-sectional area using Equation (1):

$$F=P \times A \tag{1}$$

Where F is the applied force (N), P is the design pressure (Pa), and A is the pipe cross sectional area (m^2) .

The force calculation is obtained from pipe parameters such as: the pipe design specification is 5.6 MPa, the outer diameter is 152.4 mm, and the thickness is 15.0 mm. The cross-sectional area of the pipe was calculated using Equation (2):

$$A=\pi \times \frac{(D_{Outer}-2t)^2}{4}$$
 (2)

Where D_0 is the outer diameter of the pipe (m) and t is the thickness of the pipe (m). So that the results of the calculation of the pipe cross-sectional area become

$$A=\pi \times \frac{(152.4-2\times15.04)^2}{4}$$

$$A = 0.01174 \text{ mm}^2$$

Therefore, the internal force can be calculated as:

 $F=P \times A$

 $F=5.6 \times 0.0117$

F = 66000N

RESULTS AND DISCUSSIONS

Hardness Results

The hardness results after PWHT can be seen in Figure 8. Hardness decreased after PWHT in all positions of the basic metal, HAZ and center of weld. Position 0° ranged from 126-174 HRB, position 120° produced a value of 122-143 HRB and position 270° had a value of 133-154 HRB. This condition indicates that there is a change in the mechanical properties of the welding joint. Figure 8 shows that the hardness value before PWHT treatment is higher, this occurs because the microstructure such as ferrite needles produces stress concentration points in the welding area.

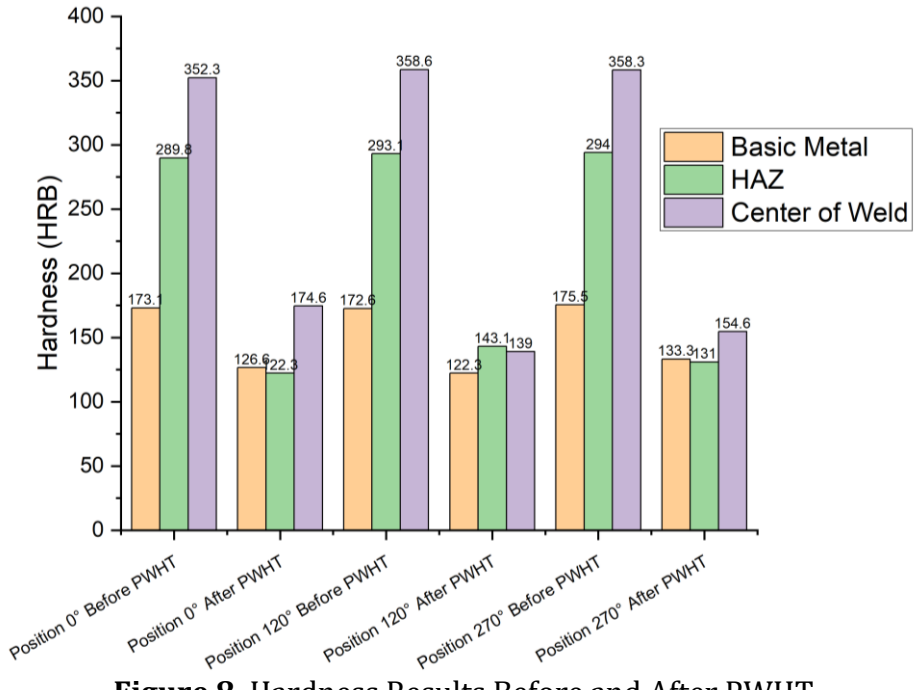


Figure 8. Hardness Results Before and After PWHT

PWHT treatment causes the microstructure to become finer, the grain size of the cementite and ferrite lamellae becomes smaller and evenly distributed, thus increasing toughness and decreasing hardness [19], [20]. The decrease in hardness occurs because at a temperature of 626°C the reinforcing phase becomes incoherent with the matrix [21]. Liu's research [22] also indicates that the density of the precipitation phase in the center of the weld is higher than in the HAZ area. The condition of reduced hardness indicates a decrease in residual stress, this occurs because when the holding time releases internal stresses due to the high temperature of the welding. The release of internal stresses results in a rearrangement of the metal structure and produces large and uniform grain sizes. Research by Gunawan et al. shows that reducing hardness will have an impact on toughness and standardize grain size so that it is safe in sulfide stress cracking, the hardness is obtained at around HAZ 143-147 HV [23].

Hydrogen Test Results

The results of the hydrogen test after PWHT can be seen in Table 2. Based on Table 2, the highest pressure produced was 3150 psi, the recorder temperature increased from 28°C to 29°C - 35°C . The recorder temperature stabilized at 31°C . The environmental temperature increased gradually from 31°C to 35°C . The high temperature increase in environmental temperature indicates the need for cooling time.

Overall, the pressure generated in the hydrogen test did not exceed the yield strength of the API 5L Gr.X65 PSL2 pipe material, which is 65,300 psi [24]. This condition indicates that the pipe did not experience failure and leakage at the welding joints. The resulting environmental temperature was <150°C, which indicates that there is no risk of hydrogen embrittlement [25]. Hydrogen testing with PWHT treatment is very risky because it will increase hydrogen traps (micro holes) which has an impact on increasing hydrogen concentration. Increasing hydrogen concentration results in a decrease in plasticity properties and crack tip propagation. In general, the cracks that occur are of the quasi-cleavage type [26]. The weak point for crack occurrence is in the Coarse-Grained

Table 2. Hydrogen Test Results

| Pressure recorder chart (Psi) | Temperature recorder (°C) | Environmental Temperature (°C) | Note | | |
|-------------------------------------|---------------------------|--------------------------------------|-------------------------------------|--|--|
| 0 | 28 | 31 | Start test pressurizing to 50% TP | | |
| U | 20 | 31 | (Test Pressure) | | |
| 1500 | 28 | 31 | Holding 15 minute | | |
| 1500 | 28 | 31 | Cont. to pressurizing to 100% TP | | |
| 3000 | 29 | 31 | 100% TP and Hold 60 min | | |
| 3000 | 29 | 32 | | | |
| 3050 | 29 | 32 | | | |
| 3100 | 30 | 33 | Holding time 100% 70 min | | |
| 3150 | 30 | 33 | End of holding and depressurized to | | |
| 3200 | 30 | 33 | design pressure | | |
| 2000 | 31 | 34 | 75% TP and holding for 15 min | | |
| 2050 | 31 | 34 | Depressurized to 50% TP | | |
| 1500 | 31 | 34 | 50% TP and holding for 15 min | | |
| 1500 | 31 | 35 | Depressurized to 0% TP | | |
| 0 | 32 | 35 | Finish test | | |

Heat Affected Zone (CGHZ) area even though the residual stress is reduced [17], but in this study based on hydrogen tests, no crack growth was found in the HAZ and basic metal areas. In this study, PWHT significantly reduced residual stresses and dislocations in the area surrounding the HAZ. This reduction in dislocations can be attributed to trapping sites, which reduce their capacity to absorb and trap hydrogen [27], [28].

Welding Size Results

The welding size simulation results can be seen in Figure 9. The maximum weld size is 6,448 mm and the minimum is 1,572 mm. The graph shows sharp fluctuations along the welding joint. The critical point occurs at the welding position 100-280 mm, where the peak drops to a minimum value. This condition can indicate insufficient weld size and can result in a decrease in the strength of the welded joint. The maximum value is used as a reference in welding pipe joints because it avoids cracks, brittle fractures, and ensures sufficient heat. In addition, the purpose of welding size analysis is for efficiency. If the welding size is too large, it will result in increased heat which directly affects the concentration of distortion stress, wasted electrode usage, and welding time.

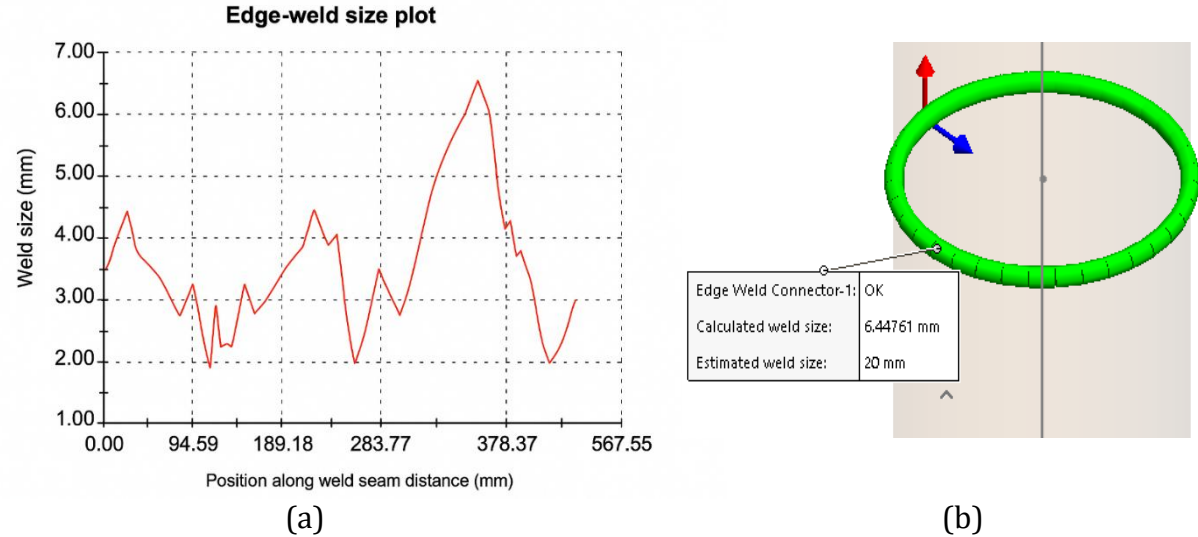


Figure 9. a) Weld Size Results b) Weld Size Details

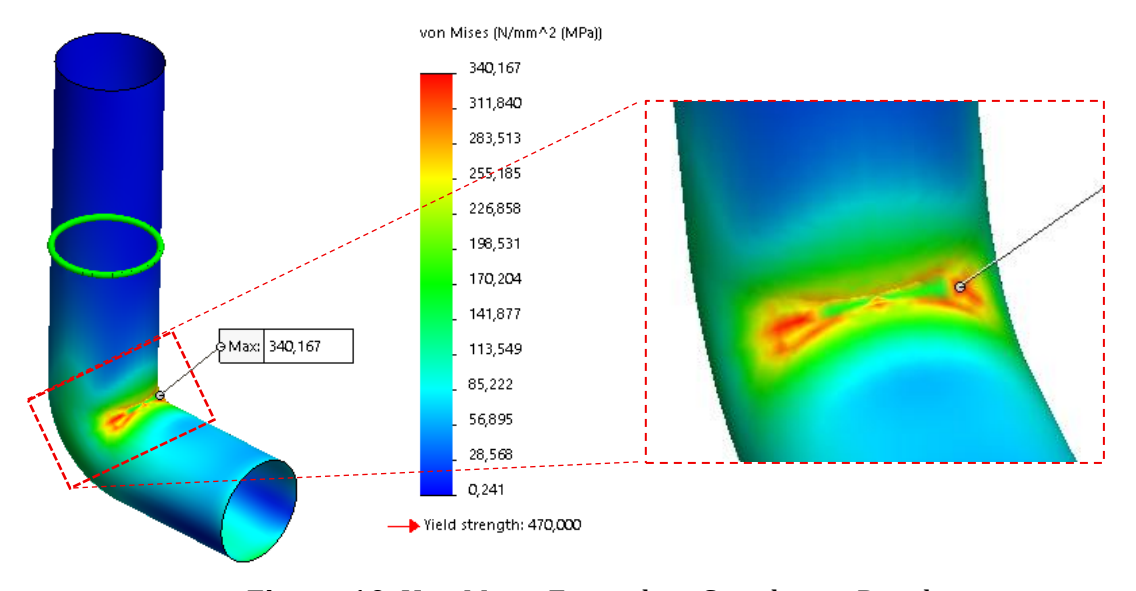


Figure 10. Von Mises Equivalent Simulation Results

The weld size results were then analyzed based on the equivalent von misses stress (Figure 10). The highest stress was generated in the pipe radius area (elbow) right at the position of the straight pipe weld joint with a value of 340.167 MPa (red section). The weld joint area is relatively very safe because it is below the yield strength value of seamless pipe material, which is 450 MPa. The highest stress generated in the elbow area is the point of stress concentration where the local stress has a higher value than the nominal value [29]. This condition often occurs in the pipe elbow area, especially on the inner wall, due to the bourdon effect and deformation due to curvature [30]. In addition, high stress in the pipe elbow can occur due to the presence of a higher bending moment and the creation of oval deformation, where this condition will create stress concentration [31].

In addition, high pressure in the pipe and the combination of bending stress will cause an increase in hoop stress because the wall cannot withstand the pressure evenly. The analysis of the forces that occur on the outside and inside of the pipe experiences tensile forces, while the radius experiences high compressive stress, so that the stress distribution will focus on the extradox and intradox. The weld sizing simulation yielded values of 1,572 to 6,448 mm. The maximum value was used as a reference to ensure adequate fusion and minimize insufficient weld size in the 100–280 mm segment. The critical peak stress of 340 MPa at the elbow radius was still below the yield stress, indicating that the weld sizing met the allowable stress criteria and ensured an elastic response under operating load conditions.

CONCLUSIONS

The purpose of this study was to analyze the hardness, hydrogen test, and welding size of seamless steel pipes with post weld heat treatment (PWHT). The resulting hardness of the basic metal, HAZ, and center of weld decreased after PWHT. The 0° position ranged from 126-174 HRB, the 120° position produced a value of 122-143 HRB, and the 270° position had a value of 133-154 HRB. The decrease in hardness indicates a decrease in residual stress and an increase in toughness. The hydrogen test indicated that the resulting pressure did not exceed the yield strength of the seamless pipe. In addition, the resulting environmental temperature was less than 150°C, which means the pipe was not at risk of hydrogen embrittlement. The welding size simulation results for the maximum value were 6.448 mm and the minimum value was 1.572 mm. The maximum value was used as a welding reference, so as to avoid brittle fracture, sufficient heat, and efficiency in electrode usage. Hydrogen and temperature test results indicate improved resistance to hydrogen embrittlement, thus improving the safety of welded joints under operating conditions. Furthermore, weld size simulation results provide a practical guideline for selecting optimal weld dimensions to maintain mechanical integrity, prevent brittle fractures, and improve electrode efficiency. Further research can expand this approach through residual stress testing using X-Ray Diffraction (XRD), HAZ morphology testing using Scanning Electron Microscopy (SEM), and fracture toughness testing.

ACKNOWLEDGEMENTS

The author would like to thank the design laboratory in the automotive department of Madiun State Polytechnic and the manufacturing laboratory in mechanical engineering, University of Merdeka Malang, which have helped the author in completing this research.

DECLARATION OF CONFLICTING INTERESTS

The authors declare that they have no potential conflicts of interest regarding the

research, authorship, and/or publication of this article.

FUNDING

The author(s) disclosed receipt of financial support for the research, authorship, and/or publication of this article.

REFERENCES

- [1] M. J. Kaiser and E. W. McAllister, "Pipeline Rules of Thumb Handbook (Ninth Edition)," Gulf Professional Publishing, 2023, pp. 1–60. doi: 10.1016/B978-0-12-822788-6.00008-6.
- [2] M. Mahmoodian, "Reliability and Maintainability of In-Service Pipelines," Gulf Professional Publishing, 2018, pp. 1–48. doi: 10.1016/B978-0-12-813578-5.00001-9.
- [3] S. Karamanos, "Structural Mechanics and Design of Metal Pipes," Elsevier, 2023, pp. 43–58. doi: 10.1016/B978-0-323-88663-5.00007-4.
- [4] G. Méndez, S. Capula-Colindres, J. Velázquez et al., "Mechanical Characterization of Resistance-Welded and Seamless API 5L X52 Pipes: A Comparative Study," *Coatings*, vol. 14, p. 343, Mar. 2024, doi: 10.3390/coatings14030343.
- [5] T. Yu, F. Zhang, L. Zhao et al., "Crack Failure Analysis of Stainless Steel Seamless Pipe," in *Advances in Machinery, Materials Science and Engineering Application IX*, IOS Press, 2023, pp. 98–103. doi: 10.3233/ATDE230446.
- [6] A. Andoko, P. Kurniawan, S. Suprayitno et al., "Residual Stress and Texture Analysis of Leaf Spring Failure," *Int. J. Technol.*, vol. 15, no. 4, p. 1162, Jul. 2024, doi: 10.14716/ijtech.v15i4.5571.
- [7] Ž. Božić, S. Schmauder, and H. Wolf, "The effect of residual stresses on fatigue crack propagation in welded stiffened panels," *Eng. Fail. Anal.*, vol. 84, pp. 346–357, Feb. 2018, doi: 10.1016/j.engfailanal.2017.09.001.
- [8] P. Kurniawan and Andoko, "Simulation of stress intensity factor and fatigue life on leaf spring failure," *AIP Conf. Proc.*, vol. 2991, no. 1, p. 020015, Jun. 2024, doi: 10.1063/5.0198716.
- [9] P. Kurniawan, Darto, and Jumiadi, "Simulation of stress and hysteresis curves on vehicle drive gear transfer failure with static structural and transient approaches," *AIP Conf. Proc.*, vol. 2991, no. 1, p. 020025, Jun. 2024, doi: 10.1063/5.0198655.
- [10] F. W. Brust and D. S. Kim, "Processes and Mechanisms of Welding Residual Stress and Distortion," Z. Feng, Ed., in Woodhead Publishing Series in Welding and Other Joining Technologies. , Woodhead Publishing, 2005, pp. 264–294. doi: 10.1533/9781845690939.2.264.
- [11] H. Diantoro, J. Jumiadi, and I. Widyastuti, "Analysis of The Effect of Post Weld Heat Treatment (PWHT) on The Hardness and Corrosion Rate of SMAW Welded Joints on AISI 304 Plates," *TRANSMISI*, vol. 20, no. 1, pp. 19–26, Mar. 2024, doi: 10.26905/jtmt.v20i1.12716.
- [12] M. Stewart and O. T. Lewis, "Pressure Vessels Field Manual," M. Stewart and O. T. Lewis, Eds., Gulf Professional Publishing, 2013, pp. 1–48. doi: 10.1016/B978-0-12-397015-2.00001-9.
- [13] A. Baisukhan, N. Naksuk, P. Insua et al., "Influence of Post-Weld Heat Treatment on Mechanical Properties and Microstructure of Plasma Arc-Welded 316 Stainless Steel," *Materials*, vol. 17, no. 15, Art. no. 15, Jan. 2024, doi: 10.3390/ma17153768.
- [14] P. Moore and G. Booth, "The Welding Engineers Guide to Fracture and Fatigue," in *The Welding Engineers Guide to Fracture and Fatigue*, P. Moore and G. Booth, Eds., Oxford: Woodhead Publishing, 2015, pp. 185–195. doi: 10.1533/9781782423911.2.185.

- [15] I. Kusminah, D. Anggara, D. Wardani et al., "Analysis of the Effect of PWHT on the Corrosion Test of API 5L X65 Material in Submerged Arc Welding," *J. Mech. Eng. Sci. Innov.*, vol. 4, pp. 122–132, Oct. 2024, doi: 10.31284/j.jmesi.2024.v4i2.6556.
- [16] K. Ravikiran, L. Li, G. Lehnhoff et al., "Crystallographic texture before and after post weld heat treatment of high-frequency electric resistance welded API X65 linepipe," *Mater. Sci. Technol.*, p. 02670836241309815, Dec. 2024, doi: 10.1177/02670836241309815.
- [17] X. Wang, D. Wang, L. Dai et al., "Effect of Post-Weld Heat Treatment on Microstructure and Fracture Toughness of X80 Pipeline Steel Welded Joint," *Materials*, vol. 15, no. 19, Art. no. 19, Jan. 2022, doi: 10.3390/ma15196646.
- [18] H. Alipooramirabad, A. Paradowska, S. Nafisi et al., "Post-Weld Heat Treatment of API 5L X70 High Strength Low Alloy Steel Welds," *Materials*, vol. 13, no. 24, p. 5801, Dec. 2020, doi: 10.3390/ma13245801.
- [19] M. Abd Majid and M. Sarwar, "Effect of Post Weld Heat Treatment on Weld Hardness Quality of P91 Welded Pipes," *Appl. Mech. Mater.*, vol. 799–800, pp. 377–381, Oct. 2015, doi: 10.4028/www.scientific.net/AMM.799-800.377.
- [20] R. K. Aninda, S. M. Karobi, R. Shariar et al., "Effect of post-weld heat treatment on mechanical properties and microstructure in electric arc welded mild steel joints," *J. Eng. Res.*, vol. 12, no. 2, pp. 210–215, Jun. 2024, doi: 10.1016/j.jer.2023.10.012.
- [21] L. Tuz, Ł. Sokołowski, and S. Stano, "Effect of Post-Weld Heat Treatment on Microstructure and Hardness of Laser Beam Welded 17-4 PH Stainless Steel," *Materials*, vol. 16, no. 4, p. 1334, Feb. 2023, doi: 10.3390/ma16041334.
- [22] F. Liu, H. Zhao, and Z. Xu, "Effect of post-weld heat treatment on the microstructure and mechanical properties of SSFSW HVDC AlSiMgMnCu alloy," *J. Mater. Res. Technol.*, vol. 21, pp. 3686–3702, Nov. 2022, doi: 10.1016/j.jmrt.2022.11.012.
- [23] G. dwi haryadi, R. Ismail, and M. Haira, "Pengaruh Post Weld Heat Treatment (Pwht) dengan Pemanas Induksi Terhadap Sifat Mekanik dan Struktur Mikro Sambungan Las Shield Metal Arc Welding (Smaw) pada Pipa API 5l X52," *ROTASI*, vol. 19, p. 117, Sep. 2017, doi: 10.14710/rotasi.19.3.117-124.
- [24] "API 5L Pipe Specification PSL1 & PSL2," UNIASEN. Accessed: Jul. 02, 2025. [Online]. Available: https://uniasen.com/standards/api-5l/
- [25] A. S. Tazedakis, N. Voudouris, E. Dourdounis et al., "Qualification of High-Strength Linepipes for Hydrogen Transportation based on ASME B31.12 Code," EITEP Institute, Mar. 2021. Accessed: Jul. 02, 2025. [Online]. Available: https://www.pipeline-journal.net/articles/qualification-high-strength-linepipes-hydrogen-transportation-based-asme-b3112-code
- [26] L. Briottet, I. Moro, and P. Lemoine, "Quantifying the hydrogen embrittlement of pipeline steels for safety considerations," *Int. J. Hydrog. Energy*, vol. 37, pp. 17616–17623, Nov. 2012, doi: 10.1016/j.ijhydene.2012.05.143.
- [27] C. Huang, C. Cui, R. Niu, F. Lu, C.-Y. Wu, X. Zhu, H. Lu, Y. Zhang, P.-Y. Liu, B. Dong, Y.-H. Sun, H. Wang, W. Li, H.-W. Yen, A. Guo, J. M. Cairney, E. Martínez-Pañeda, and E. Y.-S. Chen, "Strong hydrogen trapping by tangled dislocations in cold-drawn pearlitic steels," *Acta Mater.*, vol. 296, p. 121231, Sep. 2025, doi: 10.1016/j.actamat.2025.121231.
- [28] H. Yu, A. Díaz, X. Lu, B. Sun, Y. Ding, M. Koyama, J. He, X. Zhou, A. Oudriss, X. Feaugas, and Z. Zhang, "Hydrogen Embrittlement as a Conspicuous Material Challenge—Comprehensive Review and Future Directions," *Chem. Rev.*, vol. 124, no. 10, pp. 6271–6392, May 2024, doi: 10.1021/acs.chemrev.3c00624.
- [29] S. Wang, R. Shi, J. Wu, C. Yang, and H. Liu, "Investigation on Optimization of Finite Element Model for Stress Analysis of 12Cr1MoV Main Steam Pipeline Elbow," *Crystals*, vol. 15, no. 3, Art. no. 3, Mar. 2025, doi: 10.3390/cryst15030207.

- [30] S. D. Vijaya Kumar, S. Karuppanan, V. Perumal, and M. Ovinis, "Failure pressure prediction of high-strength steel pipe bend considering pipe and corrosion geometry," *Discov. Appl. Sci.*, vol. 6, no. 4, p. 165, Mar. 2024, doi: 10.1007/s42452-024-05812-6.
- [31] S. S and R. Venkatasamy, "Stress Analysis of Oval Pipe Bend with Attached Pipe using Finite Element Analysis," *Asian J. Res. Soc. Sci. Humanit.*, vol. 6, p. 1868, Jan. 2016, doi: 10.5958/2249-7315.2016.01135.7.